

Characterization of an Off-Body Channel at 2.45 GHz in an Underground Mine Environment

Moulay El Azhari¹, Mourad Nedil^{1, *}, Ismail Ben Mabrouk²,
Khalida Ghanem³, and Larbi Talbi⁴

Abstract—Underground mines are challenging environments for off-body wireless communication, since the signal propagation is majorly affected by small scale and large scale fading. The use of multiple antennas at the transmitter and the receiver sides is a known technique to combat fading and enhance capacity. In this paper, the channel parameters of a 2×2 Multiple-Input Multiple-Output (MIMO) off-body system are investigated in an underground gold mine and compared to the Single-Input Single-Output (SISO) system parameters. Measurement campaigns were conducted using monopole antennas at a center frequency of 2.45 GHz for both Line Of Sight (LOS) and None Line of Sight (NLOS) scenarios. The measured frequency responses are converted into impulse responses through an Inverse Fourier Transform (IFT). The results show that for a constant transmitted power, the path loss exponents at NLOS are smaller than their counterpart values at LOS. The channel capacity values decrease as the propagation distance increases and when the link is obstructed at NLOS. The RMS delay spread is generally increasing with distance for both LOS and NLOS situations. When a fixed Signal-to-Noise Ratio (SNR) is assumed, MIMO topologies improved the SISO capacity by roughly 8 bps/Hz. The channel characterization results demonstrate that the MIMO configurations provided a remarkable improvement in terms of capacity, coherence bandwidth, and time delay spread compared to the SISO topologies.

1. INTRODUCTION

In recent years, the research community has focused much attention on underground wireless communication. It has been established that underground environments are challenging for wireless communication because of the high path loss and dynamic channel condition [1, 2]. Furthermore, many research studies were directed towards the implementation of wireless communication systems in underground mines aiming to increase the safety of the miners [3]. In fact, underground mines are known to be environments into which many fatal events may occur. During these accidents, hazardous conditions could rise, including toxicants such as carbon monoxide (CO), flammable gases such as methane (CH₄), fires, and insufficient oxygen concentration [3]. Hence, advanced and appropriate technologies that improve the underground general safety need to be developed, especially those related to the sensing process and monitoring.

Lately, wireless sensors are finding increasingly important applications in health care, military, firefighting, sports, police and security agencies, and entertainment [4–6]. Many of these envisioned applications involve body-worn sensors, resulting in the so-called wireless body area networks (WBAN) [7]. WBAN refers to the wireless communication technology encompassing the propagation

Received 15 June 2015, Accepted 12 August 2015, Scheduled 15 August 2015

* Corresponding author: Mourad Nedil (mourad.nedil@uqat.ca).

¹ Underground Communications Research Laboratory, University of Quebec in Abitibi-Temiscamingue (UQAT), Val d'Or, Canada. ² Sensor Networks and Cellular Systems (SNCS) Research Center, University of Tabuk, Tabuk, Saudi Arabia. ³ Division Architecture des Systèmes, Centre de Développement des Technologies Avancées, Algiers, Algeria. ⁴ Department of Computer Science and Engineering, University of Quebec in Outaouais (UQO), Canada.

at the On-body, Off-body, and In-body channels [8, 9]. In the On-body channel, the transmitter and receiver are on the human body surface; whereas in the in-body channel the transmitter is within the body [9]. In the Off-body channel, which is the topic of this paper, the transmitter is located on the body, whilst the receiver is in the vicinity of the body. In this area, the WBAN technology could be implemented to display the toxic gases' levels to the miners or to deliver information to the command station, in a timely manner. This allows a fast detection of potential problems and hence eases the decision making, improving the miners' safety and health. However, in a mine environment, the reliability of the wireless link is affected by short-term and long-term fading caused mainly by multipath communication and shadowing [9]. Moreover, the human body has a high dielectric constant with a high loss tangent and low conductivity at the microwave frequency band [9]. Consequently, the gain and radiation efficiency of the antenna can be deteriorated when it is operated on the human body [9]. Hence, to fully understand the propagation mechanism on and around the body, it is essential to characterize the WBAN channel through the determination of its parameters, such as the path loss, impulse response, RMS delay spread, and coherence bandwidth.

In our previous works [8, 10], the Off-body performance of a single input single-output (SISO) system in a mine gallery was evaluated. It was shown that the path loss values for the SISO channel are significant, with a path loss exponent higher than that of free space for LOS scenarios [8, 10]. The SISO capacity, which was determined to be between 6 and 10 bps/Hz, might not be good enough for a robust communication system. Consequently, to take advantage of the multipath richness of the mine environment, MIMO technique has been chosen as a mean to increase capacity and enhance the channel performance [11, 12]. In fact, MIMO systems were widely investigated in underground mines for conventional radio transmission [13, 14].

In this paper, the performance of a MIMO Off-body channel inside a mine gallery is investigated and compared to the SISO technique. The characterization and capacity evaluation of the 2×2 MIMO Off-body channels are examined in underground environment at the 2.45 GHz band. Monopole antennas were used in the measurements' campaigns for LOS and NLOS scenarios. First, the channel impulse responses are evaluated for different locations of the access points relative to the body. The path loss is then determined and plotted for different distances between the transmitter and the receiver. The coherence bandwidth and RMS delay spread are derived and discussed. Additionally, the Shannon SISO capacity, which is defined as the maximum data rate transmittable over a channel with arbitrarily small error probability [15], is calculated from measurements. For the 2×2 MIMO systems, the maximum theoretical capacity was determined assuming either a fixed SNR or a fixed transmitted power. When a variable SNR and a fixed transmitted power are assumed, the capacity results include both the effects related to the multipath richness as well as the path loss [16, 17]. On the other hand, when the effect of the path loss is isolated by fixing the SNR, the capacity results reflect the effect of the multipath richness of the environment [16–18]. Hence, this paper studies the effect of a strong LOS component and multipath propagation on the MIMO link capacity. Results on the SISO and MIMO capacities are detailed in references [18–21].

To the best of the authors' knowledge, no study of the MIMO Off-body channel characterization in underground mines has been reported yet in the literature. The rest of the paper is organized as follows: Section 2 describes the measurements' setup used to characterize the underground Off-body channel. Section 3 presents results from different measurement scenarios to determine and discuss several channel parameters. Finally, Section 4 discusses the conclusions and results derived from this study.

2. MEASUREMENT SETUP

The measurement campaign was conducted in the CANMET gold mine near Val d'Or in Canada as represented in Fig. 1 and Fig. 2. The environment mainly consists of very rough and dusty walls, floor, and ceiling. The temperature is about 6°C in a highly humid environment. There is mining machinery few meters away from the measurement setup; the ceiling includes many metal rods and is covered with metal screens.

In order to characterize the Off-body MIMO propagation channel in this mine gallery at the 2.45 GHz band, the transmitting antennas were placed at a fixed position in the middle of the mine pathway. The receiving antennas were placed on the right chest side of a 1.80 m, 75 kg male subject

wearing a miner’s outfit. A 2×2 MIMO monopole antenna set was used in the measurements. Both transmitting and receiving antennas are separated by a half wavelength distance (of approximately 6 cm). During the measurements, 6 data snapshots were collected in the frequency domain at each distance, from a distance of 1 m through 5 m away from the transmitter, as shown in Fig. 3. The transmitting and receiving antennas were connected to the two ports of the previously calibrated vector network analyzer (VNA). At each snapshot, the transmission coefficient S_{21} values were recorded for 6401 frequency samples around the center frequency of 2.45 GHz, as illustrated in Table 1. The noise floor for the measurements was considered at -90 dBm [8, 10].

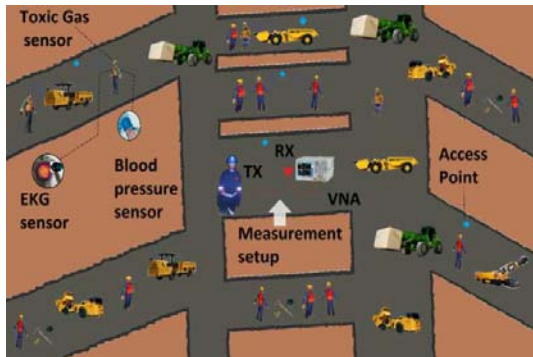


Figure 1. Representation of the BAN system in a mine environment. **Figure 2.** Measurement setup.

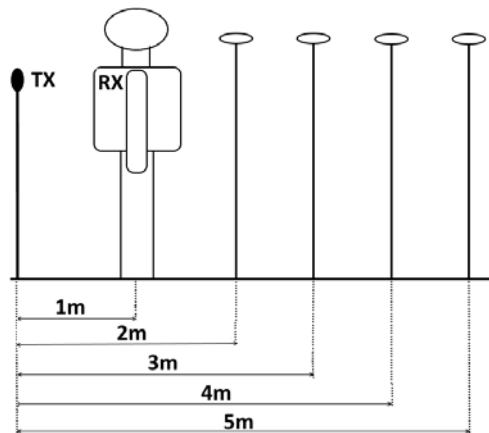


Figure 3. Measurement scenario.

Table 1. Measurement parameters.

Equipment	Parameter	Value
VNA (of type Anritsu)	Center frequency	2.45 GHz
	Number of points	6401
	Sweep time	Auto
	Calibratio	Full-2-port (Tx power = -10 dBm)
Human body	Gender	Male
	Height	180 cm
	Weight	75 kg
Antenna	Type	Monopole
	Distance to body	5–10 mm
	Orientation	Head to Head

3. RESULTS AND DISCUSSION

3.1. MIMO Channel Model

The MIMO input-output relationship between m transmit and n receive antennas is described by the following equation [18]:

$$Y = HX + N \quad (1)$$

where X is the $[m \times 1]$ transmitted vector, Y the $[n \times 1]$ received vector, N the receive additive white Gaussian noise (AWGN) vector, and H the $n \times m$ channel matrix which for the case of the 2×2 MIMO considered channel is reduced to:

$$H = \begin{bmatrix} h_{11} & h_{12} \\ h_{21} & h_{22} \end{bmatrix} \quad (2)$$

where h_{ij} is the complex random variable that represents the complex sub-channel gain from the j th transmitting antenna to the i th receiving antenna. In our measurements, the values of the S_{21} parameters correspond to the different h_{ij} values.

3.2. Channel Impulse Response

An inverse Fourier transform was applied to the measured frequency-domain S_{21} sets of values in order to obtain the sub-channels' impulse responses. Then, the MIMO channel impulse response is calculated as the arithmetic mean of all sub-channels' impulse responses, for each distance. Fig. 4 depicts the impulse responses for a transmitter-receiver (Tx-Rx) separation of 2 m. It can be seen that the LOS signal generally carries the highest power among the multipath received signals. Moreover, some multipath signals are added constructively and some other components are added destructively by the MIMO antenna set up. Hence, it is worth noting that some of these MIMO averaged multipath amplitudes are higher than their SISO counterparts, while other MIMO multipath' amplitudes are smaller.

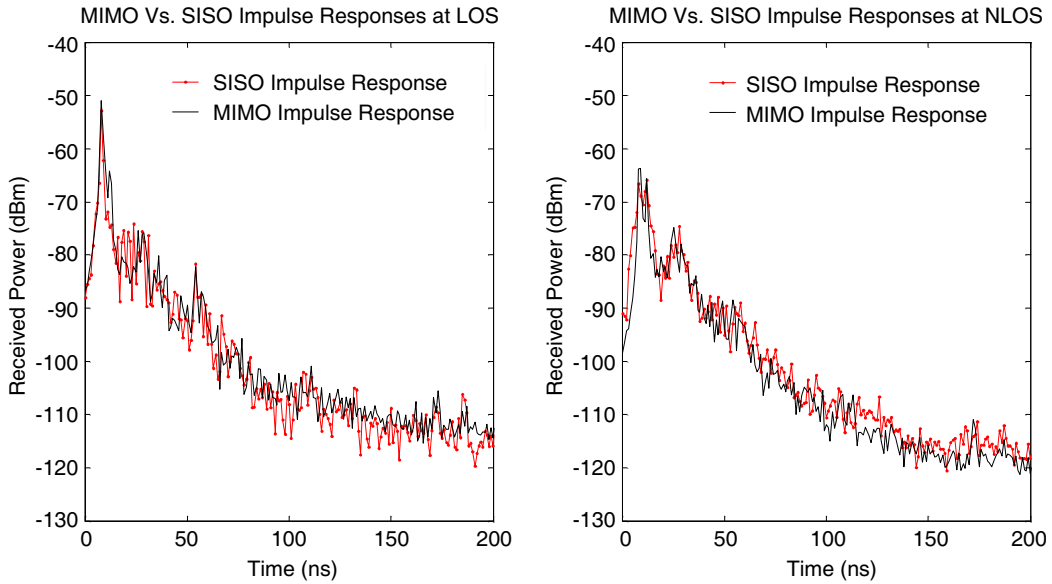


Figure 4. MIMO vs. SISO impulse responses for a Tx-Rx separation of 2 m.

3.3. Path Loss

The path loss (PL) is defined as the ratio of the transmitted power to the local average of the received power [13], and it is represented as follows:

$$PL_{dB} = 20 \text{Log}_{10} (\xi \{G_{x,y,f}\}) \quad (3)$$

where $G_{x,y,f}$ is the spatial sub-channel path gain at a given frequency sample and ξ the expectation operator over all receiving antennas, transmitting antennas, frequencies, and snapshots [13].

For the SISO system, the path loss was obtained by averaging the path gains over the different frequencies, samples, and snapshots [4]; thus, as a special case of Eq. (3), it reduces it to the following expression [4]:

$$PL(d(p)) = -20 \log_{10} \frac{1}{N_s N_f} \sum_{j=1}^{N_s} \sum_{n=1}^{N_f} |H_j^p(n)| \quad (4)$$

where $PL(d(p))$ denotes the path loss at a given position p (with Tx-Rx separation $d(p)$), and N_s and N_f are the total numbers of snapshots and frequency samples, respectively. $H_j^p(n)$ stands for the measured S_{21} parameter corresponding to the p th position, j th snapshot, and n th frequency sample [4].

When expressed in terms of the Tx-Rx distance, the path loss can be modeled as [13]:

$$PL(d) = PL_{dB}(d_0) + 10 \cdot \alpha \cdot \log_{10} \left(\frac{d}{d_0} \right) + X \quad (5)$$

where $PL(d_0)$ is the mean path loss at the reference distance d_0 , d the distance where the path loss is calculated, α the path loss exponent which is determined by using the least square linear regression analysis for instance, and X a zero mean Gaussian variable (in dB) representing the shadowing effect.

The path loss results obtained in the case of MIMO and SISO systems are plotted in Fig. 5 and Fig. 6.

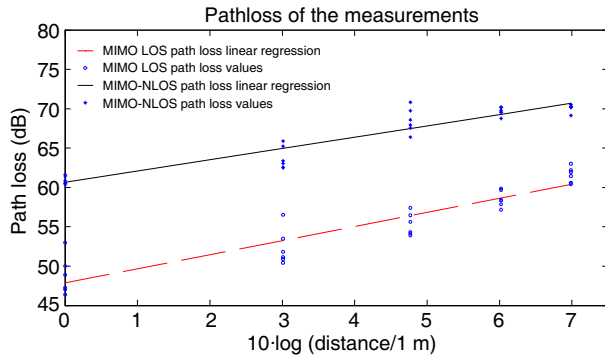


Figure 5. Path loss values and their linear regression for the MIMO channel.

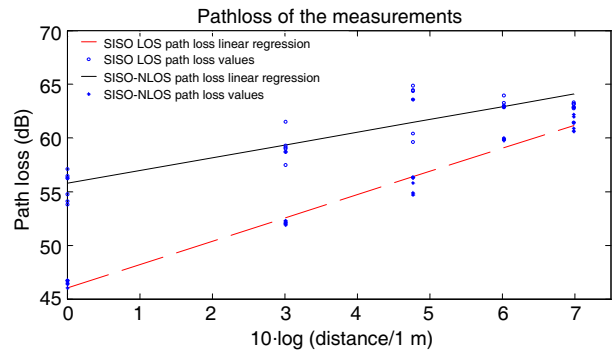


Figure 6. Path Loss values and their linear regression for the SISO channel [8, 10].

From the above linear regression analysis, the path loss exponent α , for LOS configurations, is found to be close to the free-space path loss exponent (which is equal to 2). Table 2 shows that the path loss exponents for NLOS scenarios are smaller than those of the corresponding LOS situations; whereas, the PL values are larger in NLOS compared to LOS, due to the shadowing effect of the human obstacle. The signal is damped slower at NLOS configurations due to the constructive multipath power additions. This result is expected because the path loss exponents are typically low for Off-body links in NLOS cases as discussed in [22–24]. Moreover, the path loss results for NLOS scenarios present a more significant dispersion (up to 6 dB) than those of LOS scenarios. This phenomenon is due to the randomness of the creeping wave and multi-path propagation [22–24].

Mostly, the effect of the human obstruction is less severe than the obstruction caused by the mining machinery seen in [13] and [25], where the path loss exponent was increased at NLOS.

Table 2. PL exponent values for the different off-body channel configurations.

Configuration	MIMO		SISO	
Parameters	LOS	N-LOS	LOS	N-LOS
PL-exponent	1.79	1.43	2.16	1.19

3.4. RMS Delay Spread and Coherence Bandwidth

The RMS delay spread is a parameter that quantifies the time dispersive properties of a multipath channel; it was determined using the following expression [26]:

$$\tau_{\text{RMS}} = \sqrt{\overline{\tau^2} - \bar{\tau}^2} \quad (6)$$

where $\overline{\tau^2}$ and $\bar{\tau}$ represent the second moment of the power delay profile (PDP) and the mean excess delay, respectively. This parameter is defined as follows [26]:

$$\bar{\tau} = \frac{\sum_k a_k^2 t_k}{\sum_k a_k^2} = \frac{\sum_k p(t_k) t_k}{\sum_k p(t_k)} \quad (7)$$

where $p(t_k)$ denotes the power of the k th path and t_k its corresponding delay. The parameter a_k^2 is the overall time average of the squared magnitude of the channel impulse response. Herein, six measurements are averaged.

On the other hand, the coherence bandwidth, which is the well-known statistical measure of the range of frequencies over which the channel can be considered flat, was calculated for a 50% correlation by adopting the following usual approximation [26].

$$B_c \simeq \frac{1}{5\tau_{\text{RMS}}} \quad (8)$$

Figure 7 and Fig. 8 represent the achieved RMS delay spread and coherence bandwidth vs. distance, for LOS and NLOS scenarios respectively. It is observed that the RMS delay spread increases whereas the coherence bandwidth decreases with the distance.

The MIMO topology results demonstrate an improvement in terms of RMS delay spread and coherence bandwidth compared to the previously published SISO results [8, 10]. At LOS, the MIMO RMS delay spread values vary from 7.40 ns to 16.6 ns and the coherence bandwidth span the values from 12.0 MHz to 27.1 MHz. The previously published SISO RMS delay spread values were between 14.7 ns and 66.2 ns, and the coherence bandwidths in the range of 3.00 to 13.6 MHz for the SISO topologies at LOS [10]. In the case of NLOS, the MIMO' RMS delay spread results in Fig. 8, which span the values from 15.6 ns to 45.1 ns, are decreased and the coherence bandwidth is increased, compared to the SISO results reported in [10]. This could be explained by the observed decrease in the secondary multipath signals' powers compared to the first arriving multipath signal power, when using MIMO. On the other hand, the LOS component is significantly higher (relative to the multipath powers) in MIMO configurations, which explains the decrease in the RMS delay spread for MIMO compared to the SISO case.

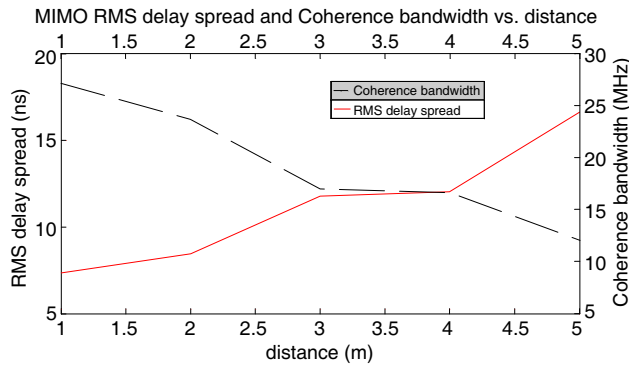


Figure 7. MIMO RMS delay spread and coherence bandwidth vs. distance for LOS measurements.

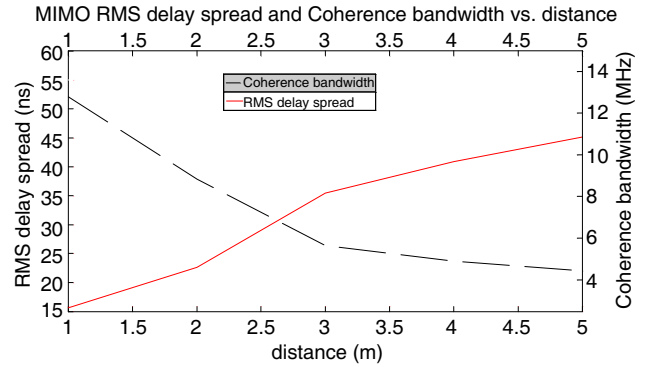


Figure 8. MIMO RMS delay spread and coherence bandwidth vs. distance for NLOS measurements.

3.5. Channel Capacity for a Constant Transmitted Power

Channel ergodic capacities are plotted in Figs. 9 and 10 for the case of a constant transmitted power. The SISO channel capacity is calculated using the Shannon formula [19]:

$$C_{\text{SISO}} [\text{bps/Hz}] = \log_2 (1 + \rho |H|^2) \tag{9}$$

where H is the normalized channel response and ρ the average signal to noise ratio (SNR). Similarly, channel capacity with MIMO configuration is computed using the following formula [18]:

$$C_{\text{MIMO}} [\text{bps/Hz}] = \log_2 \left(\det \left[\mathbf{I}_n + \frac{\text{SNR}_{av}}{m} \mathbf{H}\mathbf{H}^* \right] \right) \tag{10}$$

where \mathbf{H} is the normalized $m \times n$ channel response ($m \geq n$), SNR_{av} the average signal to noise ratio, and $*$ represents the complex conjugate transpose. In our case, \mathbf{H} matrix is normalized such that the average of the square of its Frobenius norm over all instances equals to the product of its dimensions ($\langle \|\mathbf{H}\|_F^2 \rangle = nm$) [18].

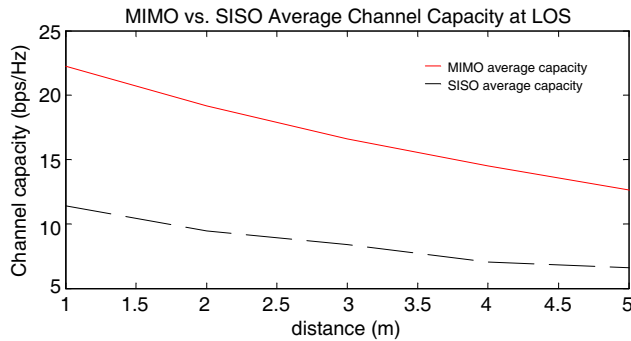


Figure 9. MIMO vs. SISO average capacity at LOS assuming a constant transmitted power.

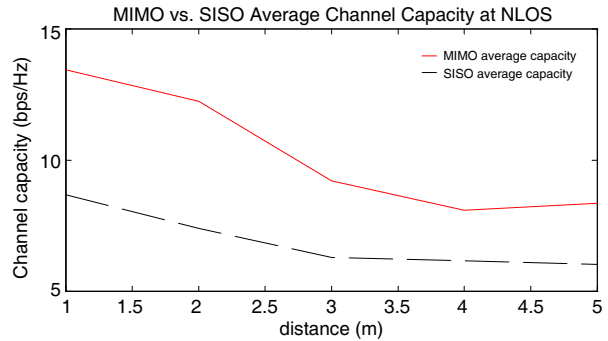


Figure 10. MIMO vs. SISO average capacity at NLOS assuming a constant transmitted power.

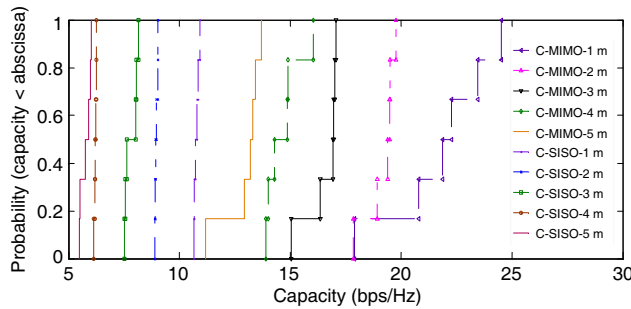


Figure 11. MIMO and SISO capacity CDFs for the five off-body channel' distances for a constant transmitted power at LOS case.

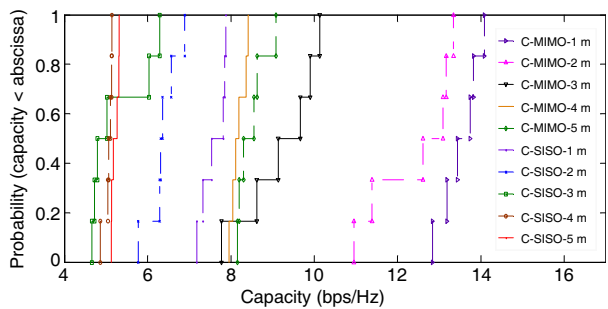


Figure 12. MIMO and SISO capacity CDFs for the five off-body channel' distances for a constant transmitted power at NLOS case.

When a constant transmitted power is assumed, the channel capacity at a certain probability level decreases with distance; this result is illustrated in Figs. 11 and 12. Figs. 9 and 10 emphasize the same result that the average capacity decreases with distance. In fact, the smaller distances correspond to the higher received average powers and hence higher average SNRs which have a direct impact on the capacity as given in Eqs. (9) and (10). Moreover, it is clear from these figures that the use of MIMO configuration offers an improvement in capacity compared to the SISO case. This result is valid for both scenarios (LOS and NLOS). Furthermore, the LOS configurations exhibit higher capacities compared to the NLOS situation due to the stronger SNR at the receiver.

3.6. Channel Capacity for a Constant SNR

The channel capacities are recalculated using Eqs. (9) and (10) assuming a constant SNR to show the effect of the multipath richness on the capacity, while canceling the path-loss effect [18]. The H matrix is normalized such that at each realization, the square of its Frobenius norm is equal to the product of its dimensions ($\|H\|_F^2 = nm$) [27, 28].

In this case, a SNR value of 20 dB was assumed, which is more than enough to guaranty that the noise will not affect the analyzed results. In fact, the measurements exhibit much higher SNR values, making a SNR value of 20 dB a reasonable choice. The CDF graphs of the MIMO capacity at LOS in Fig. 13 show that for probability levels smaller than 80%, the 1 m and the 5 m capacities are higher than the other capacities. This is due to the fact that, at the LOS case, the multipath' components are more important for these distances. On the one hand, the reflected signals' powers are more significant when the distance is small. On the other hand, the number of multipath components is increased with distance, whereas their powers become significantly lower compared to the LOS component.

For the NLOS case, the capacity values are more important for 2 m, 3 m, and 5 m distances for all probability levels as illustrated in Fig. 14. The multipath richness, which becomes more significant at these distances and the generally lesser correlation at NLOS, play an important role in capacity enhancement. Moreover, a maximum variation of 2 bps/Hz is observed when comparing the capacity' values at the different distances and snapshots. Additionally, an average capacity improvement of 8.5 bps/Hz is achieved for MIMO, compared to the corresponding SISO capacity of 6.6582 bps/Hz, as derived using an SNR value of 20 dB in Eq. (9). It can be concluded that the multipath richness is a significant factor in capacity improvement.

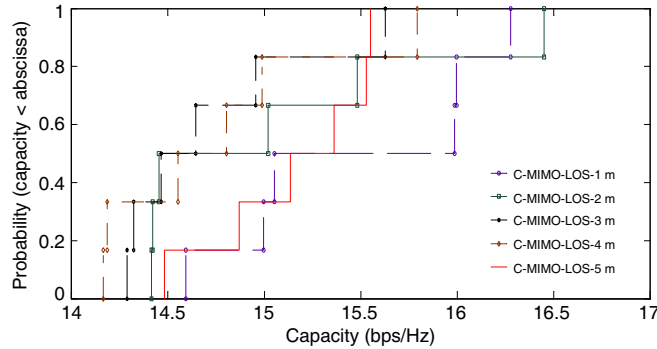


Figure 13. MIMO capacity CDFs for the five off-body channel' distances assuming a constant SNR at LOS.

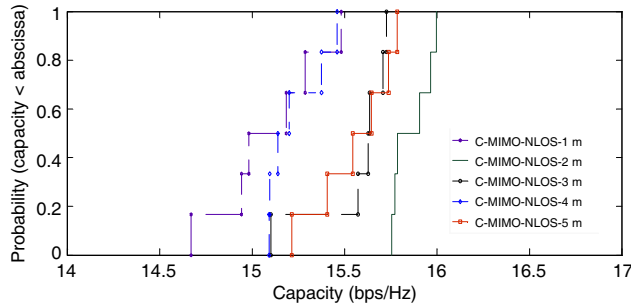


Figure 14. MIMO capacity CDFs for the five off-body channel' distances assuming a constant SNR at NLOS.

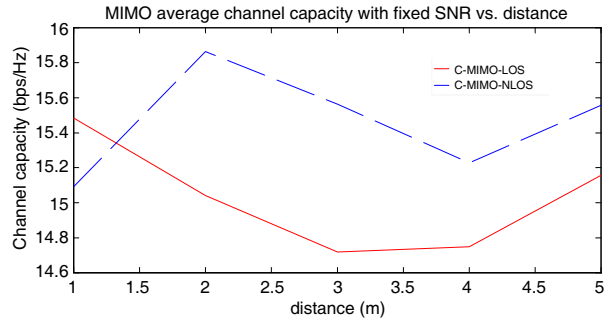


Figure 15. MIMO average channel capacities with a fixed SNR vs. distance.

4. CONCLUSION

In this study, a 2×2 MIMO Off-body channel has been characterized in a mine gallery using monopole antennas. It was observed that the path-loss exponent is close to that of free space for LOS situations, and decreases at NLOS due to constructive multipath additions. When the transmitted power is fixed, the capacity decreases with the increase in distance due to the decrease in the average SNR. The NLOS capacity is lower than that of a corresponding LOS situation when the effect of the PL is taken into consideration. When the SNR is fixed, an improvement of about 8.5 bps/Hz is achieved through the use of MIMO compared to the SISO configurations, which proves the significance of the multipath richness in the channel capacity enhancement. Moreover, for a fixed SNR, the capacity generally increases at NLOS compared to the corresponding LOS capacity due to a lower correlation. In LOS cases, there is a tradeoff between the increase of the multipath richness and the decrease of the multipath powers; the capacity values reflect this tradeoff, with capacity peaks at the 1 m and 5 m distances. Comparing the results of the channel capacity using the two methodologies reveals the fact that the path loss has a greater effect on capacity than the multipath richness. In conclusion, MIMO topologies provided a remarkable improvement in terms of capacity, coherence bandwidth, and time delay spread compared to the SISO topologies.

Presently, there are several open research problems. First, the effect of directivity and polarization was not emphasized in this study. Hence a similar study, analyzing the effect of radio-wave polarization in off-body MIMO systems operating inside a mine, needs to be addressed in future work. The next open problem that future research work needs to consider is the exploration of other bands such as the UWB and the 60 GHz band, which would allow exploiting a considerably larger bandwidth. Different diversity schemes should be investigated as a way to combat fading and improve performance. Finally, there is a need to study correlation at both the transmitter and the receiver.

REFERENCES

1. Li, L., M. C. Vuran, and I. F. Akyildiz, "Characteristics of underground channel for wireless underground sensor networks," *Proc. Med-Hoc-Net'07*, Corfu, Greece, Jun. 2007.
2. Sun, Z. and I. F. Akyildiz, "Underground wireless communication using magnetic induction," *IEEE ICC 2009 Proceedings*, 1–5, Jun. 2009.
3. Raheem, S. R., "Remote monitoring of safe and risky regions of toxic gases in underground mines: A preventive safety measures," Postgraduate Diploma Thesis Report, African Institute for Mathematical Sciences (AIMS), South Africa, 2011, [Online], available: <http://users.aims.ac.za/~soliu/soliu.pdf>.
4. Gao, A.-M., Q. H. Xu, H.-L. Peng, W. Jiang, and Y. Jiang, "Performance evaluation of UWB on-body communication under WiMAX off-body EMI existence," *Progress In Electromagnetics Research*, Vol. 132, 479–498, 2012.
5. Torre, P. V., L. Vallozzi, H. Rogier, M. Moeneclaey, and J. Verhaevert, "Reliable MIMO communication between firefighters equipped with wearable antennas and a base station using space-time codes," *Proceedings of the 5th European Conference on Antennas and Propagation (EUCAP)*, Vol. 10, 2690–2694, Apr. 2011.
6. Khan, I., P. S. Hall, A. A. Serra, A. R. Guraliuc, and P. Nepa, "Diversity performance analysis for on-body communication channels at 2.45 GHz," *IEEE Trans. Antennas Propag.*, Vol. 57, No. 4, 956–963, Apr. 2009.
7. Chatterjee, G. and A. Somkuwar, "Design analysis of wireless sensors in ban for stress monitoring of fighter pilots," *16th IEEE International Conference on Networks*, 1–6, Dec. 2008.
8. El-Azhari, M. E., M. Nedil, I. Benmabrouk, and L. Talbi, "Off-body channel characterization at 2.45 GHz in underground mine environment," *Proc. IEEE Antennas and Propagation Society Int. Symp. (APSURSI)*, 251–252, Jul. 6–11, 2014.
9. Khan, I., "Diversity and MIMO for body-centric wireless communication channels," PhD Thesis Report, University of Birmingham, Sep. 2009, [Online], available: <http://etheses.bham.ac.uk/433/1/Khan09PhD.pdf>.

10. El-Azhari, M. E., M. Nedil, I. Benmabrouk, L. Talbi, and K. Ghanem, "Off-body LOS and NLOS channel characterization in a mine environment," *International Conference on Electrical and Information Technologies (ICEIT)*, Marrakesh, Morocco, 2015.
11. Mabrouk, I. B., L. Talbi, and M. Nedil, "Performance evaluation of a MIMO system in underground mine gallery," *IEEE Antennas Wireless Propag. Lett.*, Vol. 11, No. 11, 830–833, Jul. 2012.
12. Lienard, M., P. Degauque, J. Baudet, and D. Degardin, "Investigation on MIMO channels in subway tunnels," *IEEE J. Sel. Areas Commun.*, Vol. 21, No. 3, 332–339, Apr. 2003.
13. Mabrouk, I. B., L. Talbi, M. Nedil, and K. Hettak, "MIMO-UWB channel characterization within an underground mine gallery," *IEEE Trans. Antennas Propag.*, Vol. 60, 4866–4874, Oct. 2012.
14. Mabrouk, I. B., L. Talbi, M. Nedil, and K. Hettak, "Experimental characterization of MIMO-UWB multipath underground mine radio channels," *Antennas and Propagation Society International Symposium*, 1–2, 2012.
15. Varzakas, P., "Average channel capacity for rayleigh fading spread spectrum MIMO systems," *International Journal of Communication Systems*, Vol. 19, No. 10, 1081–1087, Dec. 2006.
16. Molina-Garcia-Pardo, J.-M., M. Lienard, P. Degauque, C. García Pardo, and L. Juan-Llacer, "MIMO channel capacity with polarization diversity in arched tunnels," *IEEE Antennas Wireless Propag. Lett.*, Vol. 8, 1186–1189, 2009.
17. Molina-Garcia-Pardo, J.-M., J.-V. Rodríguez, and L. Juan-Llacer, "Polarized indoor MIMO channel measurements at 2.45 GHz," *IEEE Trans. Antennas Propag.*, Vol. 56, No. 12, 3818–3828, Dec. 2008.
18. Khan, I. and P. S. Hall, "Experimental evaluation of MIMO capacity and correlation for narrowband body-centric wireless channels," *IEEE Trans. Antennas Propag.*, Vol. 58, No. 1, 195–202, Jan. 2010.
19. Hakan, I., "Multiple-input multiple-output system capacity: Antenna and propagation aspects," *IEEE Antennas and Propagation Magazine*, Vol. 55, No. 1, 253–273, Feb. 2013.
20. Gesbert, D., M. Shafi, D.-S. Shiu, P. Smith, and A. Naguib, "From theory to practice: An overview of MIMO space-time coded wireless systems," *IEEE J. Sel. Areas Commun.*, Vol. 21, No. 3, 281–302, Apr. 2003.
21. Goldsmith, A., S. A. Jafar, N. Jindaland, and S. Vishwanath, "Capacity limits of MIMO channels," *IEEE J. Sel. Areas Commun.*, Vol. 21, No. 5, 684–701, 2003.
22. Hamie, J., "Contributions to cooperative localization techniques within mobile wireless body area networks," PhD Manuscript, University of Nice-Sophia Antipolis, Nov. 2013.
23. Rosni, R. and R. D'Errico, "Off-body channel modelling at 2.45 GHz for two different antennas," *Proceedings of the 6th European Conference on Antennas and Propagation (EUCAP)*, 3378–3382, 2012.
24. Denis, B., N. Amiot, B. Uguen, A. Guizar, C. Goursaud, A. Ouni, and C. Chaudet, "Qualitative analysis of RSSI behavior in cooperative wireless body area networks for mobility detection and navigation applications," *21st IEEE International Conference on Electronics Circuits and Systems (ICECS)*, 834–837, Dec. 7–10, 2014.
25. Rissafi, Y., L. Talbi, and M. Ghaddar, "Experimental characterization of an UWB propagation channel in underground mines," *IEEE Trans. Antennas Propag.*, Vol. 60, No. 1, 240–246, Jan. 2012.
26. Rappaport, T. S., "Mobile radiop propagation: Small scale fading and multipath," *Wireless Communications: Principle and Practice*, 2nd Edition, Prentice Hall, 2001.
27. Svantesson, T. and J. Wallace, "On signal strength and multipath richness in multi-input multi-output systems," *Proc. IEEE Int. Conf. on Commun.*, Vol. 4, 2683–2687, May 2003.
28. Carrasco, H., R. Feick, and H. Hristov, "Experimental evaluation of indoor MIMO channel capacity for compact arrays of planar inverted-F antennas," *Microw. Opt. Technol. Lett.*, Vol. 49, No. 7, 1754–1756, Jul. 2007.